Prepubertal ovariectomy alters dorsomedial striatum indirect pathway neuron excitability and explore/exploit balance in female mice

Kristen Delevich[1,2*], Christopher D. Hall[1], and Linda Wilbrecht[1,2*]
1 Department of Psychology, University of California, Berkeley, CA 94720, USA
2 Helen Wills Neuroscience Institute, University of California, Berkeley, CA 94720, USA

*co-corresponding author

Linda Wilbrecht, PhD
Department of Psychology
University of California, Berkeley
16 Barker Hall
Berkeley, CA 94720-1650

Tel: +1.510.600.3560
wilbrecht@berkeley.edu

Kristen Delevich, PhD
Department of Integrative Physiology and Neuroscience
College of Veterinary Medicine
Washington State University
P.O. Box 647620 Pullman, WA 99164

Tel: +1.509-335-4829
kristen.delevich@wsu.edu

Abstract:

Decision-making circuits are modulated across life stages (e.g. juvenile, adolescent, or adult)—as well as on the shorter timescale of reproductive cycles in females—to meet changing environmental and physiological demands. Ovarian hormonal modulation of relevant neural circuits is a potential mechanism by which behavioral flexibility is regulated in females. Here we examined the influence of prepubertal ovariectomy (pOVX) versus sham surgery on performance in an odor-based multiple choice reversal task. We observed that pOVX females made different types of errors during reversal learning compared to sham surgery controls. Using reinforcement learning models fit to trial-by-trial behavior, we found that pOVX females exhibited lower inverse temperature parameter (β) compared to sham females. These findings suggest that OVX females solve the reversal task using a more exploratory choice policy, whereas sham females use a more exploitative policy prioritizing estimated high value options. To seek a neural correlate of this behavioral difference, we performed whole-cell patch clamp recordings within the dorsomedial striatum (DMS), a region implicated in regulating action selection and explore/exploit choice policy. We found that the intrinsic excitability of dopamine receptor type 2 (D2R) expressing indirect pathway spiny projection neurons (iSPNs) was significantly higher in pOVX females compared to both unmanipulated and sham surgery females. Finally, to test whether mimicking this increase in iSPN excitability could recapitulate the pattern of reversal task behavior observed in pOVX females, we chemogenetically activated DMS D2R(+) neurons within intact female mice. We found that chemogenetic activation increased exploratory choice during reversal, similar to the pattern we observed in pOVX females. Together, these data suggest that pubertal status may influence explore/exploit balance in females via the modulation of iSPN intrinsic excitability within the DMS.

71 **Introduction:**
72
73 As animals interact with their environment in pursuit of rewards in the form of food, water,
74 mates etc., they learn from trial and error to guide their future choices. This process involves
75 learning from positive and negative feedback and also, importantly, deciding how learned
76 information should influence choice, referred to as choice policy. Reinforcement learning (RL)
77 models (Sutton and Barto, 1998) have provided a useful framework for understanding and
78 quantifying aspects of trial-and-error learning, including choice policy. A classic RL problem that
79 hinges on choice policy is the explore/exploit tradeoff. If an animal (or any agent for that matter)
80 adopts an exploit policy, it will consistently select the highest estimated value option, but may
81 miss out on better alternative options. On the other hand, if an animal favors a more exploratory
82 choice policy, characterized by less value-dependent, more stochastic choice behavior, it may
83 discover new and better options more readily (Sutton and Barto, 1998; Daw et al., 2006).
84 Importantly, the optimal balance of exploration and exploitation may depend on the statistics of
85 the environment and/or the needs of the animal as defined by its particular physiological or
86 developmental state (Cohen et al., 2007; Frank et al., 2009; Humphreys et al., 2015; Addicott et
87 al., 2017; Lenow et al., 2017; Gopnik, 2020). In humans, choice behavior generally becomes less
88 exploratory and more exploitative during the transition from childhood to adulthood (Nussenbaum
89 and Hartley, 2019; Gopnik, 2020; Xia et al., 2020; Eckstein et al., 2021). Natural fluctuations in
90 ovarian hormones across the estrous cycle or exogenous estradiol administration have been shown
91 to regulate aspects of value-based decision making in female rats (Uban et al., 2012; Orsini et al.,
92 2021), including explore/exploit balance (Verharen et al., 2019b). These data suggest that the rise
93 in ovarian hormones at puberty could contribute to the developmental shift in choice policy during
94 adolescence in females. In previous work, we observed that pOVX altered performance in a

95 multiple choice reversal task in adult C57/Bl6 mice (Delevich et al., 2020a). Compared to intact
96 females, pOVX females showed lower ratios of perseverative to regressive errors during reversal
97 learning, but the potential underlying biological processes that contributed to this behavioral effect
98 remained unclear.

99 The DMS is implicated in the regulation of goal-directed action selection (Tai et al., 2012;
100 Nonomura et al., 2018; Matamales et al., 2020; Peak et al., 2020) and choice policy (Collins and
101 Frank, 2014), and recent work suggests that enhancing the activity of D2R(+) SPNs in the dorsal
102 striatum biases choice behavior to be more exploratory (Lee et al., 2015; Delevich et al., 2020b)
103 but see (Verharen et al., 2019a). While nuclear estrogen receptors are notably absent from the
104 dorsal striatum in adulthood (Krentzel et al., 2021), extranuclear estrogen receptors (ERα, ERβ,
105 and GPER1) localize to SPNs, glia, and the presynaptic terminals of striatal GABAergic and
106 cholinergic interneurons of adult female rats (Almey et al., 2012). At the neuronal level, estrous
107 cycle has been shown to regulate the intrinsic excitability of SPNs located within the rodent
108 striatum (Proano et al., 2018; Alonso-Caraballo and Ferrario, 2019). Studies examining the
109 influence of estrous cycle on SPN physiology have been primarily performed in rats, where SPN
110 cell types were not distinguished, but see (Tansey et al., 1983). Taken together, these findings raise
111 the question of whether pubertal status influences choice strategies employed by females by
112 modulating striatal SPN physiology. Here we focused on D2R(+) SPNs of the indirect pathway
113 (iSPNs) within the DMS, whose activity we hypothesized regulates explore/exploit balance in
114 decision making based on theoretical predictions (Collins and Frank, 2014; Dunovan and
115 Verstynen, 2016) plus genetic (Beeler et al., 2010; Kwak et al., 2014) and pharmacological (Lee
116 et al., 2015; McCoy et al., 2019) evidence.

117 In the current study, after analyzing raw behavioral data, we applied reinforcement learning
118 modeling to examine how pOVX influenced learning and choice policy processes underlying
119 performance in the odor-based reversal learning task. We next examined the influence of pOVX
120 on the intrinsic excitability of genetically identified D2R(+) SPNs within the DMS of adult female
121 mice. Finally, we chemogenetically activated D2R(+) neurons within the DMS of female mice
122 during reversal learning and applied our RL model to determine whether this manipulation
123 recapitulated the reversal learning strategy employed by pOVX females. We found that compared
124 to intact adult females, pOVX females exhibited a more exploratory choice strategy during reversal
125 learning as evidenced by a lower explore/exploit inverse temperature parameter, β. In addition,
126 D2R(+) SPN intrinsic excitability was increased in pOVX females compared to sham females.
127 Finally, chemogenetic activation of D2R(+) SPNs within the DMS promoted a more exploratory
128 choice strategy during reversal learning in intact female mice, resembling pOVX female behavior.
129 Together, these data suggest that pubertal status influences the choice strategy female mice employ
130 via the modulation of D2R(+) SPN activity.

131 **Materials & Methods:**

132 ***Animals:***

133 Female C57BL/6NCR (Charles River), Drd2-eGFP BAC (GENSAT), and D2-Cre ER43
134 (MMRC) mice were bred in-house. Drd2-eGFP BAC and D2-Cre ER43 mice were bred onto the
135 C57BL/6NCR background for at least 5 generations. All mice were weaned on postnatal day (P)21
136 and housed in groups of 2–3 same-sex siblings on a 12:12 hr reversed light:dark cycle (lights on
137 at 2200 h). All procedures were approved by the Animal Care and Use Committee of the University
138 of California, Berkeley and conformed to principles outlined by the NIH Guide for the Care and
139 Use of Laboratory Animals.

140 ***Prepubertal Ovariectomy:***

141 Prepubertal ovariectomy was performed as previously described (Delevich et al., 2020a).
142 To eliminate ovarian hormone exposure during and after puberty, ovariectomies were performed
143 before puberty onset at P25. Prior to ovariectomy (OVX) surgery, all female mice were visually
144 inspected to confirm that vaginal opening had not occurred. Prior to surgery, mice were injected
145 with 0.05 mg/kg buprenorphine and 10 mg/kg meloxicam subcutaneously and were anesthetized
146 with 1–2% isoflurane during surgery. The incision area was shaved and scrubbed with ethanol and
147 betadine. Ophthalmic ointment was placed over the eyes to prevent drying. A 1 cm incision was
148 made with a scalpel in the lower abdomen across the midline to access the abdominal cavity. The
149 ovaries were clamped off from the uterine horn, with locking forceps and ligated with sterile
150 sutures. After ligation, the ovaries were excised with a scalpel. The muscle and skin layers were
151 sutured, and wound clips were placed over the incision for 7–10 days to allow the incision to heal.
152 An additional injection of 10 mg/kg meloxicam was given 24 and 48 h after surgery. Sham control
153 surgeries were performed in which fat pads were visualized but the ovaries were not clamped,
154 ligated, or excised. Mice were allowed to recover on a heating pad until ambulatory and were post-
155 surgically monitored for 7–10 days to check for normal weight gain and signs of
156 discomfort/distress. Mice were co-housed with 1-2 siblings who received the same surgical
157 treatment. To confirm the success of prepubertal ovariectomies, necropsy was performed on a
158 subset of adult sham and ovariectomized mice to confirm that the uteri of pOVX mice were
159 underdeveloped compared to age-matched sham females (data not shown).

160 ***4 choice odor-based reversal task:***

161 Sham or pOVX mice were tested in an odor-based reversal task that has previously been
162 described in detail (Johnson and Wilbrecht, 2011; Johnson et al., 2016) as young adults (P60-P70).

163 The task is designed such that only the odor cue is predictive of reward, while spatial and
164 egocentric information is irrelevant. Briefly, mice were food restricted to ~85% body weight by
165 the Discrimination phase. Mice were habituated to the testing arena on day 1, they were taught to
166 dig for a honey nut cheerio reward in a pot filled with unscented wood shavings on day 2,
167 underwent a 4 choice odor Discrimination on day 3, and finally, were tested on Recall of the
168 previously learned odor-reward association, which was immediately followed by a Reversal phase
169 on day 4. During the Discrimination phase of the task, mice learned to discriminate among four
170 pots with different scented wood shavings (anise, clove, litsea, and thyme). All four pots were
171 sham-baited with cheerio (under wire mesh at bottom) but only one pot was rewarded (anise). The
172 pots of scented shavings were placed in each corner of an acrylic arena (12”, 12”, 9”) which was
173 divided into four quadrants. Mice were placed in a cylinder in the center of the arena, and a trial
174 started when the cylinder was lifted. Mice were then free to explore the arena and indicate their
175 choice by making a bi-manual dig in one of the four pots of wood shavings. The cylinder was
176 lowered as soon as a choice was made. If the choice was incorrect, the trial was terminated and the
177 mouse was gently encouraged back into the start cylinder. Trials in which no choice was made
178 within 3 minutes were considered omissions. If mice omitted for two consecutive trials, they
179 received a reminder: a baited pot of unscented wood shavings was placed in the center cylinder
180 and mice dug for the “free” reward. Mice were disqualified if they committed four pairs of
181 omissions. The location of the four odor scented pots was shuffled on each trial, and criterion was
182 met when the mouse completed 8 out of 10 consecutive trials correctly. 24 hours after completing
183 Discrimination, mice were tested for Recall of the initial odor Discrimination to criterion, after
184 which, mice immediately proceeded to the Reversal phase in which the previously rewarded odor
185 (anise) was no longer rewarded, and a previously unrewarded odor (clove) was now rewarded.

186 During the Reversal phase, Odor 4 (thyme) was replaced by a novel odor (eucalyptus) that was
187 unrewarded. Again, mice were run until they reached a criterion of 8 out of 10 consecutive correct
188 trials.

189 ***4 choice odor-based reversal task analysis:***

190 To compare reversal task performance across groups, trials to criterion and errors (incorrect
191 choices) were compared for each phase of the task (Discrimination, Recall, and Reversal).
192 Omission trials did not count towards trials to criterion. In addition, for the Reversal phase we
193 separated errors in which mice chose the odor that was rewarded during Discrimination (Odor 1)
194 into two types: 1) perseverative errors occurred when Odor 1 was chosen prior to the first correct
195 trial and 2) regressive errors occurred when Odor 1 was chosen after the first correct trial during
196 the Reversal phase. To compare the relative proportion of these error types within mice, we
197 calculated Reversal error bias as (perseverative – regressive errors)/(perseverative + regressive
198 errors). Therefore, a value > 1 indicates a bias for perseverative errors whereas a value < 1 indicates
199 a bias for regressive errors. Finally, we examined how quickly mice accumulated rewards after the
200 first correct trial during the Reversal phase by aligning trial histories to the first correct trial and
201 summing rewarded trials across the subsequent 8 trials. Data were fit by linear regression for each
202 group and the slope of the lines compared to determine whether groups significantly differed in
203 their rate of reward accumulation. Behavioral data from 14 of the 16 pOVX females and 10 of the
204 15 sham females presented here were included in a previously published study examining sex
205 differences of prepubertal gonadectomy on approach-avoidance behaviors, but latent decision
206 variables were not examined (Delevich et al., 2020a).

207 ***Reinforcement learning modeling of 4 choice odor-based reversal task***

We modeled Discrimination and Reversal phase behavior using a reinforcement learning model driven by an iterative error-based rule (Rescorla and Wagner, 1972; Sutton and Barto, 1998). The model uses a prediction error (δ) to update the value (V) of each odor stimulus, where δ is the difference between the experienced feedback (λ) and the current expected value (r= 100 for rewarded, r= 0 for unrewarded) scaled by a learning rate parameter (α), with 0<α<1:

$$V(t+1)_{choice} = V(t)_{choice} + \alpha \times \delta(t)$$

$$\delta(t) = r(t) - V(t)_{choice}$$

$$r(t) \begin{cases} 100 \; if \; rewarded \; choice \\ else \; 0 \end{cases}$$

Because mice exhibit innate preferences for odors, we set initial odor values to fixed parameters [v1,v2,v3,v4] for all mice tested by calculating the probability of choosing each odor during the first 4 trials of Discrimination × 100 (see Johnson et al. 2016). To model trial-by-trial choice probabilities, the stimulus values were transformed using a softmax function to compute choice probabilities based on estimated odor values, $V(O)_i$. The inverse temperature parameter (β), which we refer to in the text as the explore/exploit parameter, determined the stochasticity of the choices:

$$\sigma(V(O))_i = \frac{e^{\beta V(O)_i}}{\sum_{i=1}^{n} e^{\beta V(O)_i}}$$

For RL modeling, trial histories from Discrimination and Recall phases were concatenated to create one Discrimination phase trial history. We compared the alternative models using AIC (Watanabe, 2010) and found that the best fit model included phase-specific (non-zero) α and β parameters; all RL model comparisons for pOVX and sham females are presented in Table S1. To assess model performance, trial-by-trial behavioral data was recovered using the best fit parameters for each animal, and average recovered choices to criterion for Discrimination and

231 Reversal phases (100 simulations/animal) were plotted against the actual choices to criterion for
232 each animal.

233 ***Stereotaxic Virus Injection***

234 Female D2-Cre mice (6-8 weeks) were deeply anesthetized with 5% isoflurane (vol/vol) in
235 oxygen and placed into a stereotactic frame (Kopf Instruments; Tujunga, CA) upon a heating pad.
236 Anesthesia was maintained at 1-2% isoflurane during surgery. An incision was made along the
237 midline of the scalp and small burr holes were drilled over each injection site. Virus was delivered
238 via microinjection using a Nanoject II injector (Drummond Scientific Company; Broomall, PA).
239 Injection coordinates for DMS were (in mm from bregma): 0.90 anterior, +/-1.4 lateral, and -3.0
240 from surface of the brain. Adeno-associated viruses (AAVs) were produced by Addgene viral
241 service and had titers of $>10^{12}$ genome copies per mL. For chemogenetic manipulations, mice were
242 bilaterally injected with 0.5 uL of rAAV8-hsyn-DIO-mCherry, rAAV8-hsyn-DIO-hM3Dq-
243 mCherry, or rAAV8-hsyn-DIO-hM4Di-mCherry. Mice were given subcutaneous injections of
244 meloxicam (10 mg/kg) during surgery and 24 and 48 hours after surgery. Mice were group-housed
245 before and after surgery and 4-6 weeks were allowed for viral expression before behavioral training
246 or electrophysiology experiments.

247 ***Drugs***

248 Clozapine-N-Oxide was generously provided by the NIMH Chemical Synthesis and Drug
249 Supply Program (NIMH C-929). CNO was made fresh each day and dissolved in DMSO (0.5%
250 final concentration) and diluted to 0.1 mg/mL in 0.9% saline USP.

251 ***Electrophysiology***

252 Mice were deeply anesthetized with an overdose of ketamine/xylazine solution and
253 perfused transcardially with ice-cold cutting solution containing (in mM): 110 choline-Cl, 2.5 KCl,

254 7 $MgCl_2$, 0.5 $CaCl_2$, 25 $NaHCO_3$, 11.6 Na-ascorbate, 3 Na-pyruvate, 1.25 NaH_2PO_4, and 25 D-
255 glucose, and bubbled in 95% O_2/5% CO_2. 300 µm thick coronal sections were cut in ice-cold
256 cutting solution before being transferred to ACSF containing (in mM): 120 NaCl, 2.5 KCl, 1.3
257 $MgCl_2$, 2.5 $CaCl_2$, 26.2 $NaHCO_3$, 1 NaH_2PO_4 and 11 Glucose. Slices were bubbled with 95%
258 O_2/ 5% CO_2 in a 37°C bath for 30 min, and allowed to recover for 30 min at room temperature
259 before recording. All recordings were made using a Multiclamp 700B amplifier and were not
260 corrected for liquid junction potential. The bath was heated to 32°C for all recordings. Data were
261 digitized at 20 kHz and filtered at 1 or 3 kHz using a Digidata 1440 A system with pClamp 10.2
262 software (Molecular Devices, Sunnyvale, CA, USA). Only cells with access resistance of <25 MΩ
263 were retained for analysis. Cells were discarded if parameters changed more than 20%. Data were
264 analyzed using pClamp or R (RStudio 0.99.879; R Foundation for Statistical Computing, Vienna,
265 AT).

266 Whole-cell current clamp recordings were performed using a potassium gluconate-based
267 intracellular solution (in mM): 140 K Gluconate, 5 KCl, 10 HEPES, 0.2 EGTA, 2 $MgCl_2$, 4
268 MgATP, 0.3 Na_2GTP, and 10 Na_2-Phosphocreatine. Alexa Fluor 594 (40 µM) was added to the
269 internal solution to enable morphological confirmation of SPN identify following recording. In
270 order to block NMDA and AMPA-mediated currents, 5 µM AP5 and 25 µM NBQX were added
271 to the ACSF, respectively for intrinsic excitability data in Figure 2. For all recordings, cells were
272 allowed to stabilize for 2 min after break in and prior to any current injection. For current clamp
273 recordings to test the effect of CNO in Gq-DREADD- expressing vs. mCherry-expressing D2R(+)
274 neurons, baseline input-output curves were collected before 5 minute wash-on of 10 µM CNO.

275 ***Histology***

276 Mice were transcardially perfused with PBS followed by 4% PFA in PBS. Following 24h
277 postfixation, coronal brain slices (75 µm) were sectioned using a vibratome (VT100S Leica
278 Biosystems; Buffalo Grove, IL). To confirm viral targeting, we performed a standard
279 immunohistochemical procedure using a primary antibody against red fluorescence protein (RFP)
280 (rabbit, Rockland 600-401-379; 1:1000) to enhance the mCherry signal expressed in mice
281 transduced with rAAV8-hSyn-DIO-DREADD-mCherry or rAAV8-hSyn-DIO-mCherry. Sections
282 were counterstained with DAPI (Life Technologies; Carlsbad, CA). Images were acquired with a
283 Zeiss Axio Scan.Z1 epifluorescence microscope (Molecular Imaging Center, UC Berkeley) at 10x
284 magnification and viewed using FIJI (ImageJ). Anatomical regions were identified according to
285 the Mouse Brain in Stereotaxic Coordinates by Franklin and Paxinos and the Allen Institute Mouse
286 Brain Atlas.

287 ***Statistics and Data Analysis***

288 For comparisons between 2 groups, a t-test was used when data were normally distributed, and
289 Welch's correction was applied when variance was unequal. The D'Agostino & Pearson test was
290 used to test for normality. For experiments in which 3 groups were compared, a one-way ANOVA
291 or Kruskal Wallis test when not normally distributed was performed, followed by two-tailed
292 uncorrected Fisher's LSD or Dunn's test, respectively, for pairwise comparisons. Two-way
293 ANOVA was performed when two independent variables were examined (e.g. treatment and error
294 type), followed by uncorrected Fisher's LSD (two-tailed) for pairwise comparisons. Post-hoc
295 comparisons were not corrected, due to the limited number of planned comparisons. Throughout
296 the paper, $p=0.05$ was used as the criterion for a significant statistical difference unless noted
297 otherwise. Data are expressed as mean ± SEM unless noted otherwise.

298

299 **Results:**

300 **Prepubertal ovariectomy affects reversal learning by promoting exploratory choice policy**

301 We performed sham surgery or pOVX on female C57/Bl6 mice at postnatal day 25 (P25),
302 prior to puberty onset, and trained them in an odor-based reversal task between P60-70 (Fig. 1A).
303 The odor-based reversal task consisted of two main phases: 1) a Discrimination phase during
304 which mice learned through trial and error that one of four scented pots of wood shavings contained
305 a buried food reward and 2) a Reversal phase in which the odor-reward contingency was reversed
306 (Fig. 1B). Sham females were not staged for estrous cycle, and both groups performed similarly
307 in the Recall phase (Supplementary Fig. 1). When comparing Discrimination and Reversal, there
308 was a significant effect of task phase but not treatment on trials to reach criterion [task phase:
309 $F(1,29)= 6.31$, $p= 0.018$; treatment: $F(1,29)= 0.11$, $p= 0.74$; task phase × treatment: $F(1,29)= 0.05$,
310 $p= 0.83$] (Fig. 1C).

311 Next, we more closely examined the types of errors that mice made during Reversal. Error
312 types included those made to the previously rewarded odor, which we divided into 2 subtypes:
313 perseverative (errors made before the first correct trial) and regressive (errors made after first
314 correct trial). Perseverative errors reflect a tendency to stick to a previously learned rule, whereas
315 regressive errors reflect a failure to acquire or maintain the new rule. There was a significant
316 interaction between error type and treatment group [$F(5,145)= 2.79$, $p=0.02$] (Fig. 1D). Post hoc
317 analyses revealed that pOVX females made significantly more regressive errors compared to sham
318 females ($p= 0.03$ uncorrected Fisher's LSD). We next examined the pattern of perseverative and
319 regressive errors made by individual mice. Sham females exhibited a significantly higher ratio of
320 perseverative to regressive errors (Reversal error bias) compared to pOVX females (sham vs.
321 pOVX females: $t(29)=2.12$, $p= 0.04$) (Figure 1E). Finally, we observed that sham females

322 accumulated rewards at a significantly higher rate after the first rewarded trial compared to pOVX
323 females during Reversal but not Discrimination (Figure 1F). These data suggest that sham females
324 and pOVX females reach criterion in the reversal task using different trial-by-trial strategies.

325 We next turned to computational modeling to assess if differences observed in the Reversal
326 phase between sham and pOVX females arise from a difference in odor value updating, a
327 difference in choice policy, or a combination of both. To do so, we fit trial-by-trial behavioral data
328 with RL models and used the maximum log likelihood to determine the parameters that best fit
329 each animal's behavior. The best fit model included phase-specific parameters for the learning rate
330 α and the explore/exploit inverse temperature parameter β (Fig. 1G) (see Supplementary Table 1
331 for alternate model comparison). We found that there was a significant interaction between task
332 phase and treatment for the explore/exploit parameter β [task phase $\times$ treatment: $F(1,29) = 7.35$,
333 $p= 0.011$; task phase]. In sham but not pOVX female mice, the explore/exploit parameter was
334 significantly higher during the Reversal phase compared to Discrimination phase (sham Reversal
335 vs. Discrimination: $p<0.0001$; pOVX Reversal vs. Discrimination $p= 0.07$ uncorrected Fisher's
336 LSD) and Reversal phase explore/exploit parameter was significantly lower in pOVX vs. sham
337 females (pOVX vs. sham: $p= 0.022$ uncorrected Fisher's LSD) consistent with pOVX females
338 employing a more exploratory choice policy compared to sham females (Fig. 1H).

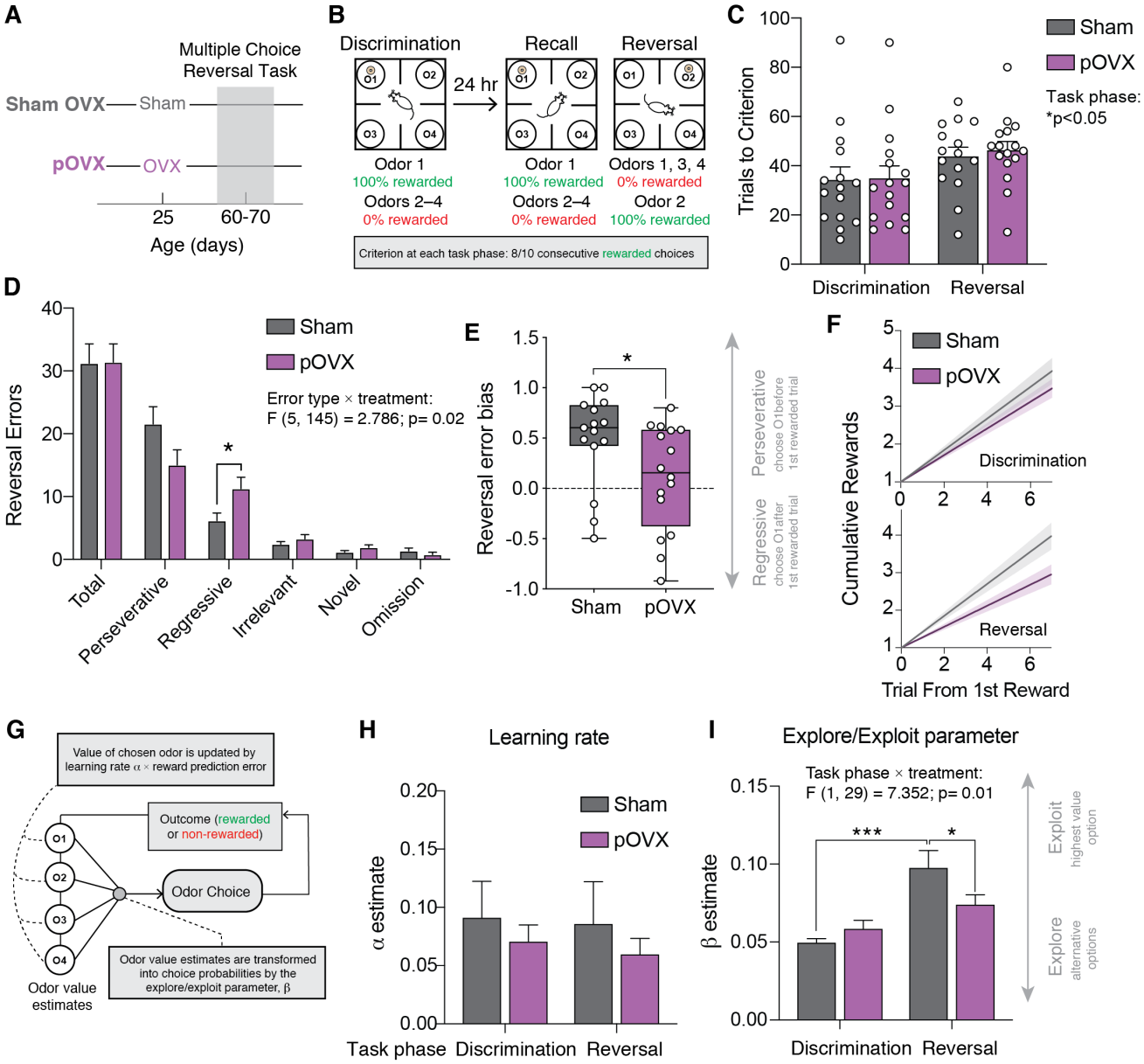

Figure 1. Prepubertal OVX is associated with more exploratory reversal learning strategy in female mice. (A) Female C57/Bl6 mice underwent OVX or sham surgery at P25 and were trained in the multiple choice reversal task in adulthood (P60-70). **(B)** Mice were trained to a criterion of 8/10 correct consecutive choices to Odor 1 during Discrimination. 24 hours later they were tested for Recall of the previous day's rule before immediately advancing to a Reversal phase during which Odor 2, rather than Odor 1, was rewarded. Reversal criterion was reached when mice made

346 8/10 correct consecutive choices to Odor 2. **(C)** There was a main effect of task phase on trials to
347 criterion but no effect of treatment (Two-way RM ANOVA main effect of task phase $F(1, 29) =$
348 6.30, $p<0.05$). **(D)** There was a significant effect of treatment and error type on the number of
349 reversal errors (Two-way RM ANOVA treatment × error type interaction: $F(5, 145) = 2.79$,
350 $p<0.05$). pOVX females made significantly more regressive errors compared to sham females
351 (11.25 ± 1.8 vs. 6.13 ± 1.2, $p<0.05$, uncorrected Fisher's LSD). **(E)** pOVX females had a
352 significantly lower Reversal error bias (perseverative – regressive errors)/(perseverative +
353 regressive errors) compared to sham females (0.11 ± 0.13 vs. 0.49 ± 0.12, $p<0.05$, unpaired t-test).
354 **(F)** Sham females accumulated rewards after the first correct Reversal trial faster than pOVX
355 females (best fit line with 95% C.I. plotted). **(G)** RL model applied to odor-based multiple choice
356 reversal task. Schematic based on (Verharen et al., 2019b). **(H)** Best-fit α learning rate estimates
357 did not significantly differ by task phase or treatment. **(I)** There was a significant interaction
358 between task phase and treatment group on the best-fit explore/exploit β parameter (Two-way
359 ANOVA task phase × treatment interaction: $F(1,29)= 7.35$, $p<0.05$). Post-hoc comparisons
360 revealed that β parameter estimates were significantly higher during Reversal compared to the
361 Discrimination phase for sham ($p<0.0001$, Sidak's multiple comparisons test) but not pOVX
362 females. In addition, Reversal phase β parameter estimates were significantly lower in pOVX
363 females compared to sham ($p<0.05$, Sidak's multiple comparisons test).

364 **Prepubertal OVX is associated with increased intrinsic excitability of D2R(+) SPNs**

365 The DMS has been implicated in action selection and determining choice policy, and
366 previous studies have found evidence that estrous cycle modulates the intrinsic excitability of
367 striatal SPNs. Furthermore, several lines of evidence suggest that D2R(+) iSPNs: 1) are modulated
368 by ovarian hormones (Le Saux and Di Paolo, 2005; Le Saux et al., 2006; Krentzel et al., 2019) and

369 2) can influence explore/exploit balance during decision making (Kwak et al., 2014; Lee et al.,
370 2015; Delevich et al., 2020b). We therefore investigated whether changes in the intrinsic
371 excitability of D2R(+) SPNs within DMS may contribute to sham vs. pOVX differences in choice
372 policy during reversal learning. We performed whole-cell current clamp recordings of visually
373 identified eGFP+ and neurons within the DMS of adult D2-eGFP transgenic female mice who
374 underwent pOVX or sham surgery and unmanipulated female mice in the presence of the
375 excitatory synaptic blockers NBQX and AP5 (Fig. 2A-C). AlexaFluor-594 was included in the
376 internal solution, and all cells included in analysis were confirmed to have spinous morphology.
377 We found a main effect of treatment on D2-eGFP(+) SPN input resistance [main effect of
378 treatment: $H= 8.76$, $p= 0.0125$] with pOVX females exhibiting higher input resistance compared
379 to sham and unmanipulated females ($p<0.05$, Dunn's multiple comparisons test) (Fig. 2D). When
380 we injected a series of positive current steps (Fig. 2E), we found that the minimum amount of
381 current necessary to trigger an action potential (rheobase) was significantly lower in pOVX
382 females compared to sham and unmanipulated females ($p<0.01$, Sidak's multiple comparisons
383 test) (Fig. 2F). In addition, there was a significant interaction between treatment and current on
384 spike output [$F(98, 1715)= 2.517$, $p<0.0001$] (Fig. 2G). While input-output curves were shifted
385 leftward in pOVX compared to sham and unmanipulated females, there was no significant effect
386 of treatment on maximum firing rate [$F(2, 18.68)= 0.10$, $p= 0.90$] (Fig. 2H). Finally, resting
387 membrane potential (RMP) did not differ across treatments [$F(2, 35)= 2.172$, $p= 0.129$] (Fig. 2I).
388 These data indicate that D2R(+) SPNs within the DMS are more intrinsically excitable in pOVX
389 females compared to unstaged sham and unmanipulated female mice.

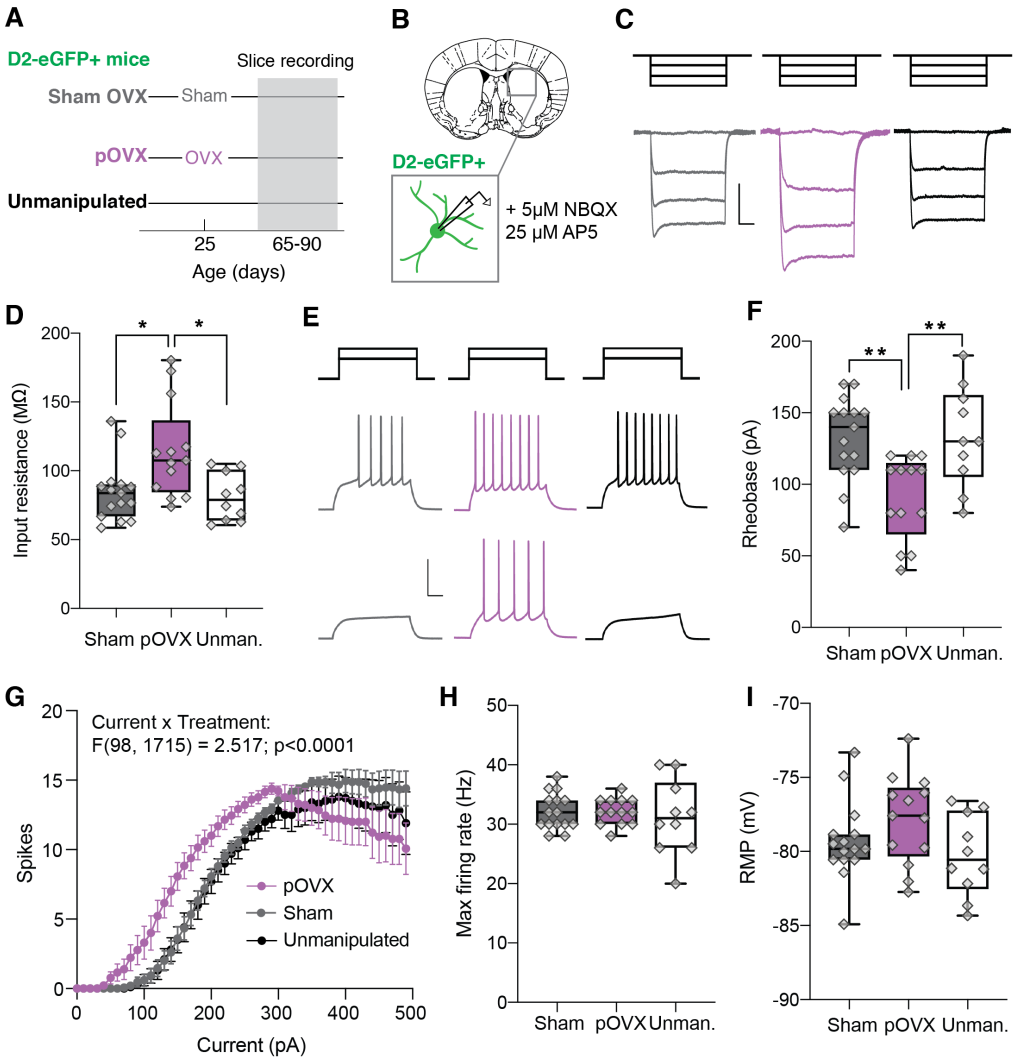

Figure 2. Prepubertal OVX increases D2R(+) SPN intrinsic excitability in the presence of synaptic blockers. (A) At P25 D2-eGFP(+) female mice underwent sham or pOVX surgery, while a third group of female D2-eGFP(+) mice received no surgery. **(B)** Whole-cell current clamp recordings were made from visually identified D2-eGFP(+) SPNs within the DMS from all groups in adulthood (P65-90). **(C)** Representative responses to negative current steps (-150, -100, -50, 0 pA) in D2R(+) SPNs from sham, pOVX, and unmanipulated females. Scale bar: 100 ms, 5 mV. **(D)** D2-eGFP(+) SPNs in pOVX female mice had higher input resistance compared to sham and unmanipulated females. **(E)** Representative responses to positive current steps (120, 180 pA) in D2R(+) SPNs from sham, pOVX, and unmanipulated females. Scale bar: 100 ms, 50 mV. **(F)**

399 Decreased rheobase of D2-eGFP(+) SPNs was observed in pOVX compared to sham and
400 unmanipulated females. **(G)** Spike number across sequential depolarizing current steps (10-500
401 pA) for D2-eGFP(+) SPNs. Increased spiking was observed in pOVX compared to sham and
402 unmanipulated females (Two-way RM ANOVA current x treatment interaction: $F(98, 1715)=$
403 2.52, $p<0.0001$). **(H)** No difference in maximum firing rate was observed across treatment groups.
404 **(I)** No difference in RMP was observed across treatment groups. *$p<0.05$, **$p<0.01$; n/N = 15/5,
405 13/5, and 10/3 for sham, pOVX, and unmanipulated mice, respectively.

406 **Chemogenetic activation of D2R(+) SPNs in DMS reduces perseverative bias and promotes**
407 **a more exploratory reversal strategy in female mice**

408 Given that OVX females exhibit a more exploratory reversal strategy and greater intrinsic
409 excitability of D2R(+) SPNs in DMS, we next asked whether experimentally increasing D2R(+)
410 SPN intrinsic excitability would similarly bias intact female mice towards increased exploration
411 during the Reversal phase. Female D2-Cre mice were bilaterally infused with 0.5 µL of Cre-
412 dependent DREADD virus (hM4Di-mCherry or hM3Dq-mCherry) and trained 4-6 weeks later in
413 the 4 choice odor-based reversal learning task (Fig. 3A). Female mice expressing Cre-inducible
414 mCherry were used to control for any effects of surgery, AAV infection, and clozapine-N-oxide
415 (CNO) administration on behavior. To examine how CNO activation of hM3Dq expressed by
416 D2R(+) SPNs in DMS alters their activity, we performed whole-cell current clamp recordings of
417 identified mCherry+ neurons in mice that expressed the excitatory DREADD hM3Dq or mCherry
418 alone (Fig. 3B). Briefly, spike output in response to depolarizing steps (0–360 pA, 20 pA steps)
419 was recorded from visually identified mCherry+ neurons in D2-mCherry or D2-hM3Dq-mCherry
420 expressing SPNs in DMS (Fig. 3A-D). Next, 10 µM CNO was bath-applied for 5 minutes and
421 spike output to the same sequential series of depolarizing current steps was recorded (Fig. 3A-D).

There was no significant interaction between current step and drug on spike output in D2-mCherry expressing SPNs [Two-way RM ANOVA, current x drug: F(18,36)=0.89, p=0.59] (Fig. 3C) but there was a significant interaction between current and drug on spike output in D2-hM3Dq-mCherry SPNs [Two-way RM ANOVA, current x drug: F(18,36)=3.93, p=0.0002] (Fig. 3D). Finally, there was a significant interaction between virus and drug on rheobase [Two-way RM ANOVA F(1,4)= 16.0, p=0.016] (Fig. 3E).

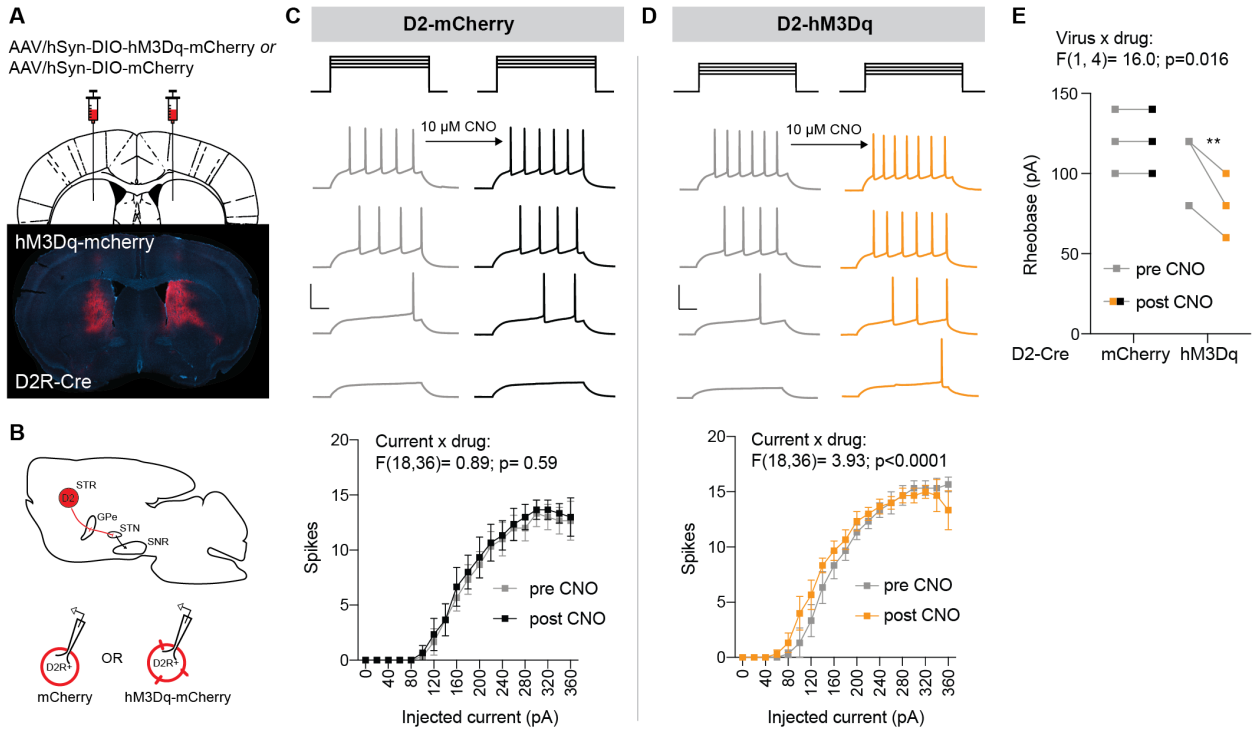

Figure 3. CNO increases intrinsic excitability of hM3Dq-expressing iSPNs. (A) Schematic of injection and representative brain section showing hM3Dq-mCherry expression in the DMS of D2-Cre mouse. **(B)** Schematic of indirect pathway expression (sagittal view) and whole-cell patch-clamp configuration of mCherry+ or hM3Dq-mCherry+ iSPNs in female D2-Cre mice. **(C)** Top panel: representative responses to positive current steps (100, 120, 140, 160 pA) in mCherry+ iSPNs before and after CNO wash on. Scale bar: 100 ms, 50 mV. Bottom panel: no significant interaction between current step and CNO treatment on spike output in D2R(+) mCherry-

435 expressing iSPNs. **(D)** Top panel: representative responses to positive current steps (100, 120, 140,
436 160 pA) in hM3Dq-mCherry+ iSPNs before and after CNO wash on. Scale bar: 100 ms, 50 mV.
437 Bottom panel: significant interaction between current step and CNO treatment on spike output in
438 D2R(+) mCherry-expressing iSPNs (Two-way ANOVA current step × drug, $p<0.0001$). **(E)**
439 Summary of CNO wash on effect on rheobase (Two-way ANOVA virus × drug, $p<0.05$).

440 Prior to Discrimination training all mice received i.p. injections of saline (Fig. 4A) and
441 learned through trial and error that one of four presented odors indicated the location of a buried
442 food reward. Mice completed the Discrimination task phase when they selected the rewarded odor
443 (Odor 1) on 8/10 consecutive trials. Twenty-four hours later, all groups were administered CNO
444 (1.0 mg/kg, i.p.) and tested for their recall of discrimination learning followed immediately by a
445 Reversal phase in which Odor 1 was no longer rewarded and Odor 2 became rewarded. There was
446 a significant effect of task phase on trials to criterion [Reversal vs. Discrimination; $F(1,17)= 16.58$,
447 $p= 0.0008$] but no significant effect of virus [$F(2,17) = 0.37$, $p= 0.69$] or interaction between virus
448 and task phase [$F(2,17)= 0.09$, $p=0.92$] (Fig. 4B). While there was no significant effect of
449 chemogenetic manipulation on Reversal phase trials to criterion, we found a significant interaction
450 between virus and error type during Reversal [$F(10,85)= 2.721$, $p= 0.006$] (Fig. 4C) that was absent
451 during Discrimination when mice were on saline (Supplementary Figure 2). D2-hM3Dq mice
452 made significantly fewer perseverative errors compared to D2-mCherry ($p= 0.015$, uncorrected
453 Dunn's test) and D2-hM4Di groups ($p= 0.028$, uncorrected Fisher's LSD) and made significantly
454 more regressive errors compared to D2-hM4Di mice ($p= 0.03$, uncorrected Fisher's LSD) (Fig.
455 4C). We next examined whether chemogenetic manipulation of D2R(+) neurons in the DMS
456 altered Reversal error bias within mice. There was a significant effect of virus on Reversal error
457 bias ($H= 9.06$, $p= 0.005$ Kruskal-Wallis test), with D2-hM3Dq mice having a significantly lower

458 Reversal error bias compared to D2-mCherry (p=0.019 uncorrected Dunn's test) and D2-hM4Di
459 groups (p= 0.005 uncorrected Dunn's test) (Fig. 4D), consistent with a greater tendency to make
460 regressive errors compared to perseverative errors. This data suggests that chemogenetic activation
461 of D2R(+) neurons in the DMS produced a pattern of reversal phase choice behavior that was
462 similar to the effect seen in pOVX mice.

463 Finally, we applied RL modeling to determine whether similar changes in decision-making
464 parameters might explain the pattern of reversal behavior we observed in pOVX female mice and
465 D2-hM3Dq female mice. Fitting the same RL model (task phase-specific α and β parameters; see
466 Methods) we found that there was no significant interaction between virus and task phase on
467 learning rate α [$F(2,17)= 0.49$, $p=0.62$] (Fig. 4E), but there was a significant interaction between
468 virus and task phase for the explore/exploit parameter β [$F(2,17)= 4.09$, $p=0.035$] (Fig. 4F). The
469 Reversal phase explore/exploit parameter was significantly lower in D2-hM3Dq mice compared
470 to D2-mCherry (p=0.0003 uncorrected Fisher's LSD) and D2-hM4Di (p= 0.0095 uncorrected
471 Fisher's LSD) (Fig. 4F). These data suggest that chemogenetic activation of D2R(+) neurons
472 within DMS biases choice strategy in female mice to be more exploratory during reversal learning.
473 Moreover, chemogenetic activation of D2R(+) neurons within the DMS produced behavior in
474 female mice that mimicked the behavioral pattern seen in OVX females, including a reduction in
475 Reversal error bias during reversal learning and a reduced explore/exploit β parameter consistent
476 with a less exploitative, more exploratory choice policy. Taken together with evidence that D2R(+)
477 iSPNs within the DMS are more intrinsically excitable in pOVX compared to sham females, these
478 data support a model whereby pOVX biases reversal learning strategy towards exploration by
479 modulating iSPN intrinsic excitability within DMS (Fig. 5).
480

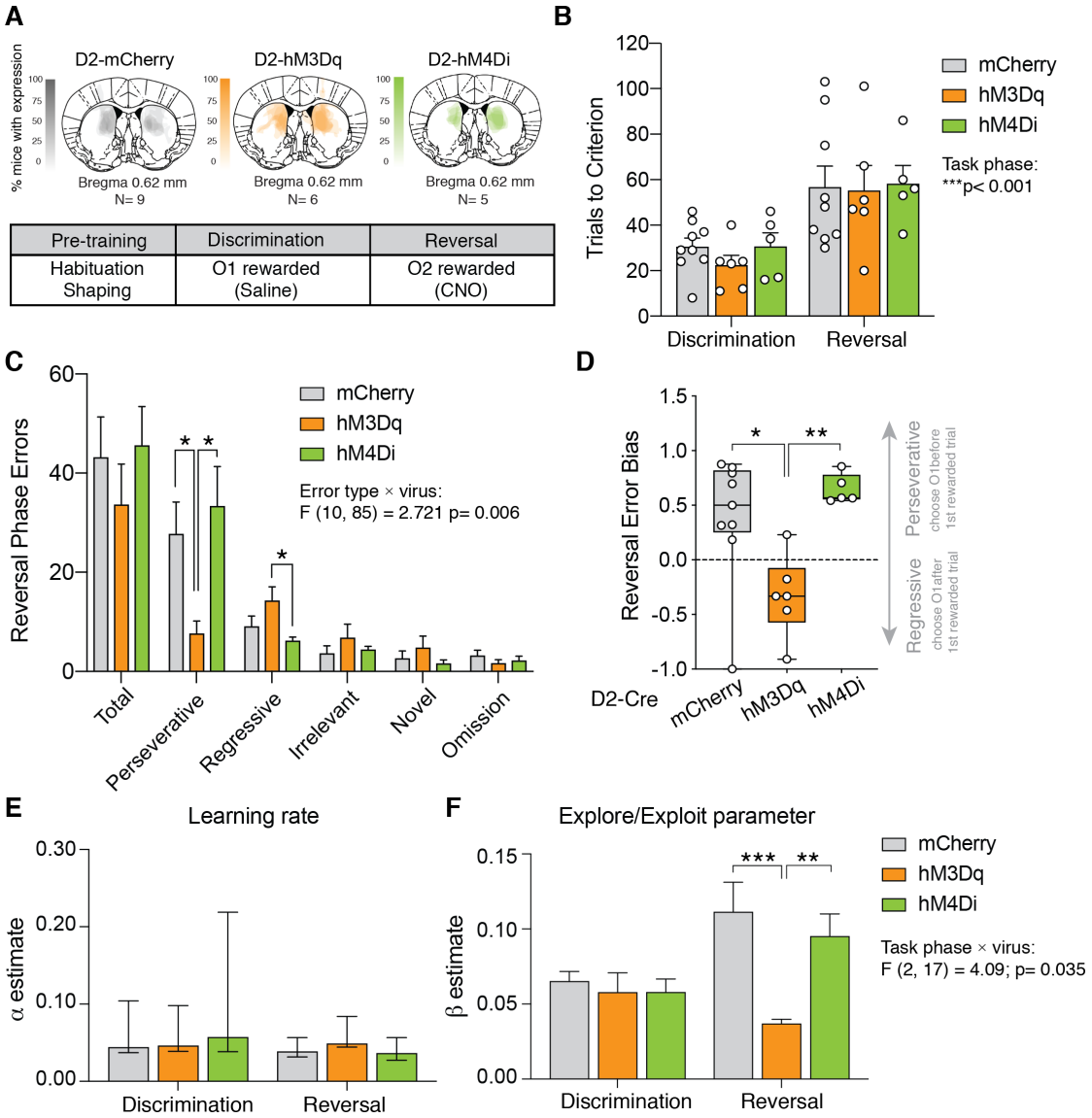

Figure 4. Chemogenetic activation of D2R(+) neurons in DMS promotes a more exploratory reversal strategy in intact female mice. (A) Top panel: schematic illustrating injection site and viral spread female D2-Cre DIO-mCherry (N=9), DIO-hM3Dq (N=6), and DIO-hM4Di (N=5) mice. Bottom panel: summary of behavioral training. **(B)** There was a main effect of task phase but no effect of virus on trials to criterion (Two-way RM ANOVA main effect of task phase: $F(2,17)= 16.58$, $p<0.001$). **(C)** There was a significant interaction between error type and virus on reversal errors (Two-way RM ANOVA error type × manipulation interaction: $F(10,85)= 2.72$,

488 p<0.01) with D2-hM3Dq mice making fewer perseverative errors (p<0.05, uncorrected Fisher's
489 LSD) compared to D2-mCherry and D2-hM4di mice and more regressive errors compared to D2-
490 hM4di mice (p<0.05, uncorrected Fisher's LSD). **(D)** There was a main effect of virus on Reversal
491 error bias (W=9.06, p<0.01 Kruskal-Wallis test), with D2-hM3Dq mice showing reduced bias for
492 perseverative errors compared to D2-mCherry (p<0.05, uncorrected Dunn's test) and D2-hM4Di
493 mice (p<0.01, uncorrected Dunn's test). **(E)** Best-fit α learning rate did not significantly differ by
494 task phase or virus. **(F)** There was a significant interaction between task phase and treatment group
495 on the best-fit explore/exploit parameter β (Two-way ANOVA task phase x treatment interaction:
496 F(2,17)= 4.09, p<0.05). Post-hoc comparisons revealed that β parameter estimates were
497 significantly higher during Reversal compared to Discrimination phase for D2-mCherry mice
498 (p<0.01, uncorrected Fisher's LSD) but not D2-hM3Dq mice (p=0.28, uncorrected Fisher's LSD).
499 In addition, Reversal phase β parameter estimates were significantly lower in D2-hM3Dq mice
500 compared to D2-mCherry and D2-hM4Di mice. *p<0.05, **p<0.01, ***p<0.001.

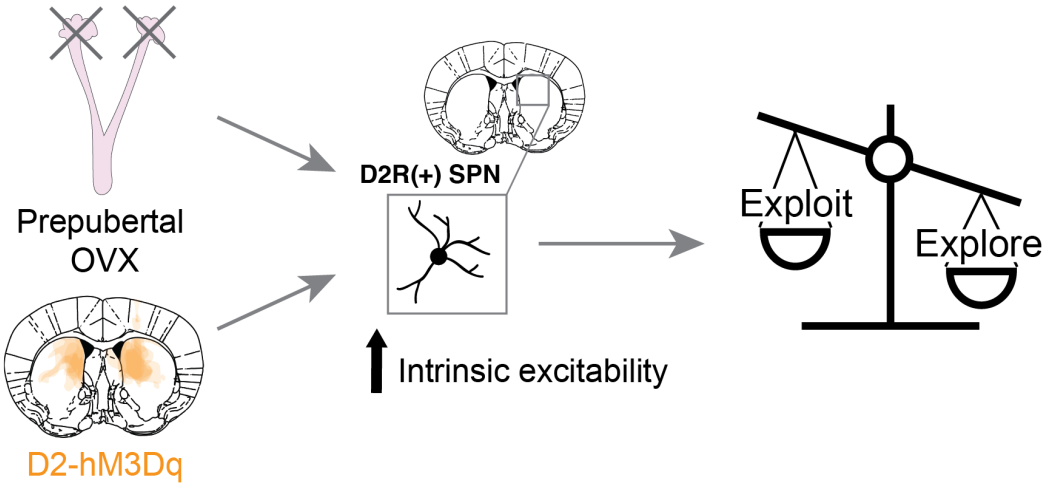

501

502 **Figure 5. Results summary.** Both pOVX and chemogenetic activation of D2R(+) neurons within
503 the DMS are associated with increased intrinsic excitability of iSPNs. In turn, both manipulations
504 are associated with less perseverative, more exploratory choice strategy during reversal learning.

While indirect, the convergent behavioral effects of pOVX and chemogenetic activation of DMS D2R(+) neurons suggest that the increased intrinsic excitability of iSPNs in the DMS of pOVX mice could contribute to the altered reversal strategy observed. Future experiments should perform *in vivo* recording of D2R(+) SPNs and/or chemogenetic manipulation experiments in pOVX females to probe the relationship between altered D2R(+) SPN intrinsic properties and reversal learning strategy on a trial-by-trial basis.

Discussion:

We found that pOVX altered how female mice solved a reversal learning task. Using RL models fit to trial-by-trial behavioral data, we found that pOVX mice exhibited a more exploratory choice policy during reversal learning than sham controls, captured by a lower inverse temperature β parameter. This difference in exploratory choice behavior was accompanied by increased intrinsic excitability of D2R(+) iSPNs in the DMS, a region that is implicated in regulating action selection and choice policy. We then sought to mimic this effect using chemogenetics. We demonstrated that chemogenetic activation of D2R(+) neurons *in vitro* similarly enhanced iSPN intrinsic excitability in slices from female brains. In addition, activation of DMS D2R(+) neurons *in vivo* decreased the ratio of perseverative to regressive errors and promoted exploratory choice captured by a lower inverse temperature β parameter. Together, these data suggest that two distinct manipulations: pOVX and hM3Dq activation converged on similar behavioral effects through a shared mechanism of enhancing DMS iSPN intrinsic excitability.

Our data are consistent with studies that manipulate D2Rs and model choice policy. Germline D2R knockout (Kwak et al., 2014), systemic D2R antagonist administration (Eisenegger et al., 2014), and intrastriatal D2R antagonist infusion (Lee et al., 2015) are each associated with more exploratory choice policy. However, none of these studies could rule out the contribution of

530 presynaptic D2 autoreceptors, which is important given the apparent role of tonic dopamine in
531 modulating explore/exploit balance (Beeler et al., 2010; Humphries et al., 2012; Cinotti et al.,
532 2019), but see (Costa et al., 2014). Our chemogenetic manipulation experiments (which do not
533 infect D2R(+) dopamine axon terminals) clearly demonstrate that activation of D2R(+) neurons
534 within DMS is sufficient to bias performance towards exploration.

535 We speculate that there are two likely circuit mechanisms downstream of D2R(+) iSPNs
536 that may be responsible for promoting exploratory choice policy. The first involves local lateral
537 connections from iSPNs to direct pathway SPNs (dSPNs) and the second involved the interface of
538 the direct and indirect pathways in basal ganglia output centers such as the substantia nigra pars
539 reticulata (SNr). One recent study showed that systemic injection of the D2R antagonist raclopride
540 induced dopamine-dependent transcriptional activation in iSPNs that opposed the activation of
541 dSPNs, suggesting that iSPN to dSPN transmodulation is an important mechanism for behavioral
542 flexibility (Matamales et al., 2020). Therefore, it is possible that elevated iSPN activity, either
543 through pOVX or chemogenetic activation, promotes exploratory choice by dampening the
544 activity of task-relevant ensembles of dSPNs that would normally promote the selection of the
545 highest estimated-value option. Opponent mechanisms between the direct and indirect pathway at
546 convergent downstream targets are also predicted to regulate choice policy (Collins and Frank,
547 2014).

548 Studies have shown that the intrinsic properties of striatal SPNs differ between females and
549 males before puberty (Dorris et al., 2015) and in an estrous cycle-dependent manner after puberty
550 (Proano et al., 2018). Interestingly, Proano et al. found that the intrinsic excitability of accumbal
551 SPNs was significantly higher during diestrus/metestrus, when estradiol and progesterone levels
552 are low, compared to proestrus/estrus (Proano et al., 2018). This may be in keeping with our

553 observation that the intrinsic excitability of D2R(+) SPNs was higher in pOVX females compared
554 to sham females, since pOVX females lack gonadally-produced estradiol and progesterone.
555 Estradiol has also been shown to influence dopamine release and reuptake in the striatum (Calipari
556 et al., 2017), including the dorsal striatum (Becker and Beer, 1986; Becker, 1990). Recent data
557 also suggest that dopamine influences the postnatal maturation of intrinsic excitability of SPN
558 populations within the striatum (Lieberman et al., 2018). Therefore, it is possible that the changes
559 we observed in D2R(+) SPN excitability in pOVX female mice may occur by direct action on
560 SPNs or downstream of hormonal effects on presynaptic dopamine release (Lin et al., 2020).

561 There are several lines of evidence that suggest that ovarian hormones preferentially
562 modulate the activity of D2R(+) iSPNs versus D1R(+) dSPNs. OVX decreases D2 receptor
563 binding in the striatum, and estradiol or treatment with an ERβ agonist counteracts the effect of
564 OVX (Le Saux et al., 2006). The aforementioned treatments did not alter D2R mRNA expression,
565 suggesting that estradiol modulates D2R binding through a mechanism other than transcriptional
566 regulation of D2R expression. Furthermore, OVX reduces the expression of preproenkephalin,
567 which produces the endogenous opioid peptide, enkephalin, which is expressed in iSPNs (Le Saux
568 and Di Paolo, 2005). Again, the effect of OVX on preproenkephalin expression can be
569 counteracted by estradiol administration. Finally, in the nucleus accumbens core, rapid
570 enhancement of mEPSC amplitude by estradiol is inversely correlated with rheobase (Krentzel et
571 al., 2019). Given that D2R(+) SPNs typically display lower rheobase compared to D1R+ SPNs,
572 this suggests that estradiol may exert a greater effect on D2R(+) iSPNs compared to D1R(+)
573 dSPNs. However, it should be noted that the authors did not observe rapid effects of estradiol on
574 mEPSC amplitude within dorsal striatum (Krentzel et al., 2019).

575 There are several limitations to our current study that should be noted. First, we cannot
576 assume that the changes we observed in SPN intrinsic excitability are specific to the dorsomedial
577 region of the striatum or to the D2R(+) SPN cell type. Second, our evidence linking the increased
578 excitability of D2R(+) SPNs in DMS to the more exploratory choice strategy used by pOVX
579 females is correlational. In independent experiments we observed that 1) pOVX promoted
580 exploratory choice strategy during Reversal 2) pOVX is associated with elevated intrinsic
581 excitability of D2R(+) SPNs in DMS and 3) that chemogenetic activation of D2R(+) SPNs in DMS
582 promoted exploratory choice strategy during Reversal. In the future, more direct evidence could
583 be gained by performing manipulation experiments to reduce the activity of DMS D2R(+) SPNs
584 in OVX females, or by recording the activity of these same neurons in pOVX and sham females
585 during behavior. Finally, while we performed OVX prior to puberty onset, we do not know whether
586 the timing of OVX plays an important role in the observed effect on behavior and physiology. We
587 also do not know if and when hormone replacement may rescue the effects of pOVX. Future
588 studies should examine timing effects of OVX and hormone replacement on these outcome
589 measures. Still, in light of these limitations, our data suggest future lines of inquiry into the
590 relationship between puberty, ovarian hormones, SPN physiology, and choice policy in value-
591 based decision making.

592 As yet, we have not identified the mechanism by which pOVX leads to enhanced
593 excitability of D2R(+) SPNs. Ovarian hormones have been shown to regulate dendritic complexity
594 and spine density in cell types in other brain regions (Gould et al., 1990; Woolley et al., 1990;
595 Wallace et al., 2006; Chen et al., 2009; Ye et al., 2019). The dendrites of D2R(+) SPNs are enriched
596 in Kir2 family inward rectifying K+ channels (Uchimura et al., 1989; Nisenbaum and Wilson,
597 1995; Mermelstein et al., 1998; Shen et al., 2007), and a reduction in dendritic length/complexity

598 has been associated with reduced Kir2 expression and increased intrinsic excitability (Cazorla et
599 al., 2012; Sebel et al., 2017). Therefore, it would be informative to compare iSPN Kir2 channel
600 currents and dendritic morphology in sham vs. pOVX females. Finally, it is possible that the
601 increase in intrinsic excitability of the D2R(+) SPNs in pOVX females could represent a
602 homeostatic plasticity mechanism that accompanies a reduction in excitatory synaptic inputs to
603 them, but we did not measure synaptic inputs onto D2R(+) SPNs in this study.

604 There is a growing interest in understanding the mechanisms that underlie sex differences
605 in value-based decision making. A recent study showed that compared to males, female mice
606 employed a more consistent strategy while learning a two-dimensional decision-making task
607 (Chen et al., 2021). This observed tendency for female mice to constrain their decision-space align
608 with the exploitative reversal learning strategy we observed in sham females. Conversely, we
609 observed that pOVX females exhibited a markedly more exploratory reversal learning strategy,
610 sticking less to the previously rewarded odor choice and committing more regressive errors
611 compared to sham females. These findings suggest that ovarian hormones contribute to the female-
612 biased choice strategies utilized during value-based decision making. While previous studies have
613 separately provided evidence that ovarian hormones regulate the intrinsic excitability of SPNs and
614 aspects of value-based decision making, we show for the first time that pOVX alters
615 explore/exploit balance of choice strategy while also increasing the intrinsic excitability of D2R(+)
616 SPNs in the DMS. These data suggest that pubertal status may influence explore/exploit balance
617 via the modulation of SPN intrinsic excitability within the DMS and highlight a role for ovarian
618 hormones in establishing sex-specific decision-making strategies in adulthood. These data can
619 inform the basic science of decision making and the study of the many psychiatric disorders that
620 emerge after puberty and also show sex differences in their prevalence or manifestation.

Acknowledgments

We thank Yuting Zhang and Kenechukwu Okwuosa for technical assistance with mouse behavior testing. We thank Dr. Helen Bateup for feedback on the manuscript and Dr. Anne Collins and Wilbrecht lab members for helpful discussion.

Declaration of interests

The authors declare that there are not conflicts of interest.

References:

Addicott MA, Pearson JM, Sweitzer MM, Barack DL, Platt ML (2017) A Primer on Foraging and the Explore/Exploit Trade-Off for Psychiatry Research. Neuropsychopharmacol 42:1931-1939.

Almey A, Filardo EJ, Milner TA, Brake WG (2012) Estrogen Receptors Are Found in Glia and at Extranuclear Neuronal Sites in the Dorsal Striatum of Female Rats: Evidence for Cholinergic But Not Dopaminergic Colocalization. Endocrinology 153:5373-5383.

Alonso-Caraballo Y, Ferrario CR (2019) Effects of the estrous cycle and ovarian hormones on cue-triggered motivation and intrinsic excitability of medium spiny neurons in the Nucleus Accumbens core of female rats. Horm Behav 116.

Becker JB (1990) Direct Effect of 17-Beta-Estradiol on Striatum - Sex-Differences in Dopamine Release. Synapse 5:157-164.

Becker JB, Beer ME (1986) The Influence of Estrogen on Nigrostriatal Dopamine Activity - Behavioral and Neurochemical Evidence for Both Pre-Naptic and Postsynaptic Components. Behav Brain Res 19:27-33.

Beeler JA, Daw N, Frazier CRM, Zhuang XX (2010) Tonic dopamine modulates exploitation of reward learning. Front Behav Neurosci 4.

Calipari ES, Juarez B, Morel C, Walker DM, Cahill ME, Ribeiro E, Roman-Ortiz C, Ramakrishnan C, Deisseroth K, Han MH, Nestler EJ (2017) Dopaminergic dynamics underlying sex-specific cocaine reward. Nat Commun 8.

Cazorla M, Shegda M, Ramesh B, Harrison NL, Kellendonk C (2012) Striatal D2 Receptors Regulate Dendritic Morphology of Medium Spiny Neurons via Kir2 Channels. J Neurosci 32:2398-2409.

Chen CS, Ebitz RB, Bindas SR, Redish AD, Hayden BY, Grissom NM (2021) Divergent Strategies for Learning in Males and Females. Curr Biol 31:39-+.

Chen JR, Yan YT, Wang TJ, Chen LJ, Wang YJ, Tseng GF (2009) Gonadal Hormones Modulate the Dendritic Spine Densities of Primary Cortical Pyramidal Neurons in Adult Female Rat. Cereb Cortex 19:2719-2727.

Cinotti F, Fresno V, Aklil N, Coutureau E, Girard B, Marchand AR, Khamassi M (2019) Dopamine blockade impairs the exploration-exploitation trade-off in rats. Sci Rep-Uk 9.

Cohen JD, McClure SM, Yu AJ (2007) Should I stay or should I go? How the human brain manages the trade-off between exploitation and exploration. Philos T R Soc B 362:933-942.

Collins AG, Frank MJ (2014) Opponent actor learning (OpAL): modeling interactive effects of striatal dopamine on reinforcement learning and choice incentive. Psychological review 121:337-366.

Costa VD, Tran VL, Turchi J, Averbeck BB (2014) Dopamine Modulates Novelty Seeking Behavior During Decision Making. Behav Neurosci 128:556-566.

Daw ND, O'Doherty JP, Dayan P, Seymour B, Dolan RJ (2006) Cortical substrates for exploratory decisions in humans. Nature 441:876-879.

Delevich K, Hall CD, Piekarski D, Zhang YT, Wilbrecht L (2020a) Prepubertal gonadectomy reveals sex differences in approach-avoidance behavior in adult mice. Horm Behav 118.

Delevich K, Hoshal BD, Zhang Y, Vedula S, Collins AGE, Wilbrecht L (2020b) Activation But Not Inhibition of the Indirect Pathway Disrupts Choice Suppression in a Freely Moving, Multiple Choice Foraging Task. In: Available at SSRN.

706 Dorris DM, Cao JY, Willett JA, Hauser CA, Meitzen J (2015) Intrinsic excitability varies by sex
707 in prepubertal striatal medium spiny neurons. J Neurophysiol 113:720-729.
708 Dunovan K, Verstynen T (2016) Believer-Skeptic Meets Actor-Critic: Rethinking the Role of
709 Basal Ganglia Pathways during Decision-Making and Reinforcement Learning. Front
710 Neurosci-Switz 10.
711 Eckstein MK, Master SL, Dahl RE, Wilbrecht L, Collins AGE (2021) The Unique Advantage of
712 Adolescents in Probabilistic Reversal: Reinforcement Learning and Bayesian Inference
713 Provide Adequate and Complementary Models. bioRxiv:2020.2007.2004.187971.
714 Eisenegger C, Naef M, Linssen A, Clark L, Gandamaneni PK, Muller U, Robbins TW (2014)
715 Role of Dopamine D2 Receptors in Human Reinforcement Learning.
716 Neuropsychopharmacol 39:2366-2375.
717 Frank MJ, Doll BB, Oas-Terpstra J, Moreno F (2009) Prefrontal and striatal dopaminergic genes
718 predict individual differences in exploration and exploitation. Nat Neurosci 12:1062-
719 U1145.
720 Gopnik A (2020) Childhood as a solution to explore-exploit tensions. Philos T R Soc B 375.
721 Gould E, Woolley CS, Frankfurt M, Mcewen BS (1990) Gonadal-Steroids Regulate Dendritic
722 Spine Density in Hippocampal Pyramidal Cells in Adulthood. J Neurosci 10:1286-1291.
723 Humphreys KL, Lee SS, Telzer EH, Gabard-Durnam LJ, Goff B, Flannery J, Tottenham N
724 (2015) Exploration-Exploitation Strategy is Dependent on Early Experience. Dev
725 Psychobiol 57:313-321.
726 Humphries MD, Khamassi M, Gurney K (2012) Dopaminergic control of the exploration-
727 exploitation trade-off via the basal ganglia. Front Neurosci-Switz 6.
728 Johnson C, Wilbrecht L (2011) Juvenile mice show greater flexibility in multiple choice reversal
729 learning than adults. Dev Cogn Neurosci 1:540-551.
730 Johnson CM, Peckler H, Tai LH, Wilbrecht L (2016) Rule learning enhances structural plasticity
731 of long-range axons in frontal cortex. Nat Commun 7:10785.
732 Krentzel AA, Barrett LR, Meitzen J (2019) Estradiol rapidly modulates excitatory synapse
733 properties in a sex- and region-specific manner in rat nucleus accumbens core and
734 caudate-putamen. J Neurophysiol 122:1213-1225.
735 Krentzel AA, Willett JA, Johnson AG, Meitzen J (2021) Estrogen receptor alpha, G-protein
736 coupled estrogen receptor 1, and aromatase: Developmental, sex, and region-specific
737 differences across the rat caudate-putamen, nucleus accumbens core and shell. J Comp
738 Neurol 529:786-801.
739 Kwak S, Huh N, Seo JS, Lee JE, Han PL, Jung MW (2014) Role of dopamine D2 receptors in
740 optimizing choice strategy in a dynamic and uncertain environment. Front Behav
741 Neurosci 8.
742 Le Saux M, Di Paolo T (2005) Chronic estrogenic drug treatment increases preproenkephalin
743 mRNA levels in the rat striatum and nucleus accumbens. Psychoneuroendocrino 30:251-
744 260.
745 Le Saux M, Morissette M, Di Paolo T (2006) ER beta mediates the estradiol increase of D-2
746 receptors in rat striatum and nucleus accumbens. Neuropharmacology 50:451-457.
747 Lee E, Seo M, Dal Monte O, Averbeck BB (2015) Injection of a Dopamine Type 2 Receptor
748 Antagonist into the Dorsal Striatum Disrupts Choices Driven by Previous Outcomes, But
749 Not Perceptual Inference. J Neurosci 35:6298-6306.
750 Lenow JK, Constantino SM, Daw ND, Phelps EA (2017) Chronic and Acute Stress Promote
751 Overexploitation in Serial Decision Making. J Neurosci 37:5681-5689.

Lieberman OJ, McGuirt AF, Mosharov EV, Pigulevskiy I, Hobson BD, Choi S, Frier MD, Santini E, Borgkvist A, Sulzer D (2018) Dopamine Triggers the Maturation of Striatal Spiny Projection Neuron Excitability during a Critical Period. Neuron 99:540-+.

Lin WC, Delevich K, Wilbrecht L (2020) A role for adaptive developmental plasticity in learning and decision making. Curr Opin Behav Sci 36:48-54.

Matamales M, McGovern AE, Mi JD, Mazzone SB, Balleine BW, Bertran-Gonzalez J (2020) Local D2-to D1-neuron transmodulation updates goal-directed learning in the striatum. Science 367:549-+.

McCoy B, Jahfari S, Engels G, Knapen T, Theeuwes J (2019) Dopaminergic medication reduces striatal sensitivity to negative outcomes in Parkinson's disease. Brain 142:3605-3620.

Mermelstein PG, Song WJ, Tkatch T, Yan Z, Surmeier DJ (1998) Inwardly rectifying potassium (IRK) currents are correlated with IRK subunit expression in rat nucleus accumbens medium spiny neurons. J Neurosci 18:6650-6661.

Nisenbaum ES, Wilson CJ (1995) Potassium Currents Responsible for Inward and Outward Rectification in Rat Neostriatal Spiny Projection Neurons. J Neurosci 15:4449-4463.

Nonomura S, Nishizawa K, Sakai Y, Kawaguchi Y, Kato S, Uchigashima M, Watanabe M, Yamanaka K, Enomoto K, Chiken S, Sano H, Soma S, Yoshida J, Samejima K, Ogawa M, Kobayashi K, Nambu A, Isomura Y, Kimura M (2018) Monitoring and Updating of Action Selection for Goal-Directed Behavior through the Striatal Direct and Indirect Pathways. Neuron 99:1302-+.

Nussenbaum K, Hartley CA (2019) Reinforcement learning across development: What insights can we draw from a decade of research? Dev Cogn Neuros-Neth 40.

Orsini CA, Blaes SL, Hernandez CM, Betzhold SM, Perera H, Wheeler AR, Ten Eyck TW, Garman TS, Bizon JL, Setlow B (2021) Regulation of risky decision making by gonadal hormones in males and females. Neuropsychopharmacol 46:603-613.

Peak J, Chieng B, Hart G, Balleine BW (2020) Striatal direct and indirect pathway neurons differentially control the encoding and updating of goal-directed learning. Elife 9.

Proano SB, Morris HJ, Kunz LM, Dorris DM, Meitzen J (2018) Estrous cycle-induced sex differences in medium spiny neuron excitatory synaptic transmission and intrinsic excitability in adult rat nucleus accumbens core. J Neurophysiol 120:1356-1373.

Rescorla RA, Wagner AR (1972) A theory of Pavlovian conditioning: variations in the effectiveness of reinforcement and nonreinforcement. In: Classical Conditioning II: Current Research and Theory (Black A, Prokasy W, eds), pp 64-99. New York: Appleton Century Crofts.

Sebel LE, Graves SM, Chan CS, Surmeier DJ (2017) Haloperidol Selectively Remodels Striatal Indirect Pathway Circuits. Neuropsychopharmacol 42:963-973.

Shen W, Tian X, Day M, Ulrich S, Tkatch T, Nathanson NM, Surmeier DJ (2007) Cholinergic modulation of Kir2 channels selectively elevates dendritic excitability in striatopallidal neurons. Nat Neurosci 10:1458-1466.

Sutton RS, Barto AG (1998) Reinforcement learning : an introduction. Cambridge, Mass.: MIT Press.

Tai LH, Lee AM, Benavidez N, Bonci A, Wilbrecht L (2012) Transient stimulation of distinct subpopulations of striatal neurons mimics changes in action value. Nat Neurosci 15:1281-U1152.

Tansey EM, Arbuthnott GW, Fink G, Whale D (1983) Oestradiol-17-Beta Increases the Firing Rate of Antidromically Identified Neurons of the Rat Neostriatum. Neuroendocrinology 37:106-110.

Uban KA, Rummel J, Floresco SB, Galea LAM (2012) Estradiol Modulates Effort-Based Decision Making in Female Rats. Neuropsychopharmacol 37:390-401.

Uchimura N, Cherubini E, North RA (1989) Inward Rectification in Rat Nucleus Accumbens Neurons. J Neurophysiol 62:1280-1286.

Verharen JPH, Adan RAH, Vanderschuren LJMJ (2019a) Differential contributions of striatal dopamine D1 and D2 receptors to component processes of value-based decision making. Neuropsychopharmacol 44:2195-2204.

Verharen JPH, Kentrop J, Vanderschuren LJMJ, Adan RAH (2019b) Reinforcement learning across the rat estrous cycle. Psychoneuroendocrino 100:27-31.

Wallace M, Luine V, Arellanos A, Frankfurt M (2006) Ovariectomized rats show decreased recognition memory and spine density in the hippocampus and prefrontal cortex. Brain Res 1126:176-182.

Watanabe S (2010) Asymptotic Equivalence of Bayes Cross Validation and Widely Applicable Information Criterion in Singular Learning Theory. J Mach Learn Res 11:3571-3594.

Woolley CS, Gould E, Frankfurt M, Mcewen BS (1990) Naturally-Occurring Fluctuation in Dendritic Spine Density on Adult Hippocampal Pyramidal Neurons. J Neurosci 10:4035-4039.

Xia L, Master S, Eckstein MK, Wilbrecht L, Collins A (2020) Learning under uncertainty changes during adolescence. In: CogSci.

Ye ZY, Cudmore RH, Linden DJ (2019) Estrogen-Dependent Functional Spine Dynamics in Neocortical Pyramidal Neurons of the Mouse. J Neurosci 39:4874-4888.